

COMPOSITION OF INDOOR AEROSOLS AT EMPEROR QIN'S TERRA-COTTA MUSEUM, XI'AN, CHINA, DURING SUMMER, 2004

Junji Cao^{1,*}, Bo Rong², Shuncheng Lee³, Judith C. Chow⁴,
Kin-fai Ho³, Suixin Liu¹ and Chongshu Zhu¹

¹Institute of Earth Environment, Chinese Academy of Sciences, Xi'an 710054, P. R. China

²Emperor Qin's Terra-Cotta Warriors and Horses Museum, Xi'an 710054, P. R. China

³The Hong Kong Polytechnic University, Hong Kong, P. R. China

⁴Desert Research Institute, Reno, NV, USA

*Author to whom correspondence should be addressed. E-mail: cao@loess.llqg.ac.cn

Abstract Particle samples were collected in August 2004 both inside and outside Emperor Qin's Terra-Cotta Museum in Xi'an, China. Mass and chemical composition of total suspended particles (TSP, particles with aerodynamic diameter less than $\sim 30 \mu\text{m}$), $\text{PM}_{2.5}$ (particles with aerodynamic diameter $< 2.5 \mu\text{m}$) were determined. The average levels of indoor $\text{PM}_{2.5}$ and TSP were 108.4 and $172.4 \mu\text{g}\cdot\text{m}^{-3}$, respectively, with $\text{PM}_{2.5}$ constituting 62.9% of the TSP mass. Sulfate ($(32.4 \pm 6.2)\%$), organics ($(27.7 \pm 8.0)\%$), and geological material ($(12.5 \pm 3.4)\%$) dominated indoor $\text{PM}_{2.5}$, followed by ammonium ($(8.9 \pm 2.8)\%$), nitrate ($(7.0 \pm 2.9)\%$), and elemental carbon (EC, $(3.9 \pm 1.5)\%$). Particle size distribution varied with the number of tourists in the museum. The size of sulfate, organics, EC, nitrate, and ammonium was found to vary in the range of 0.43 to $3.3 \mu\text{m}$ in fraction. Ion balance indicated that the aerosol was acidic, with insufficient ammonium ions to neutralize the sulfuric and nitric acids. High concentrations of acidic aerosols will erode the Terra-cotta warriors and horses especially in the summer season with high temperature (30°C) and relative humidity (70%) and undesirable solar radiation inside the museum. More attention should be paid to protecting these precious antiques made 2000 years ago.

Keywords museum atmospheres, terra-cotta, $\text{PM}_{2.5}$, chemical composition, acidic aerosols

1. Introduction

Xi'an is a famous city of historical and cultural significance in China. It used to be the capital city of 13 Chinese dynasties totalling more than a millennium. The discovery of terra-cotta figures in Xi'an in 1974 is one of the most important archeological events of the 20th century, and has led the city to become one of the most attractive cities to tourists in China. The well-known Museum of Qin Terra-cotta Warriors and Horses ($34^\circ 44' \text{N}$, $109^\circ 49' \text{E}$) is located 30 km east of Xi'an, covering a total area of 16000 m^2 . It contains more than 7000 pottery soldiers, horses, chariots, and weapons made in the Qin Dynasty (211–246 BC). These terra-cotta artifacts have not received adequate environmental protection since they were unearthed. They are being discolored by air pollution, coupled with large variations in temperature and relative humidity, after 30 years of exposure in the exhibition halls (Zhang et al., 2002; Cao et al., 2005).

The quality of indoor air in museums is important to the preservation of antiques (Nazaroff et al., 1990; Oddy, 1994; DeBock et al., 1996). Research on the indoor-outdoor air pollution in museums has been reviewed by Baer and Banks (1985) and Brimblecombe (1990). A European multidisciplinary research project concerning museum atmospheres has been carried out in many museums, such as Correr Museum, Venice (Italy), Kunsthistorisches Museum, Vienna (Austria), Royal Museum of Fine Arts, Antwerp (Belgium) and Sainsbury Centre for Visual Arts, Norwich (UK) (Brimblecombe et al., 1999; Camuffo et al., 1999; 2001; Gysels et al., 2002). However, little is known about air quality inside Chinese museums. This paper is the first research report in this field in China. In our research study,

we measured particulate matter (PM) in Emperor Qin's Terra-Cotta Museum. Moreover, microclimate, particle number, and size distribution, as well as the chemical composition of particulate matter (PM) during August 2004 were examined to provide background information for a more comprehensive evaluation in 2005.

2. Methodology

2.1 Indoor and outdoor sampling

Three main buildings of the museum — Pit 1, Pit 2, and Pit 3 — were built over the excavated sites from 1974 to 1989. Pit 1 is the largest (14269 m^2), containing 1087 terra-cotta warriors. Two sampling sites were selected for this study inside of Pit 1, as shown in Fig. 1. Aerosol samplers were located at 1.0 m above ground level.

$\text{PM}_{2.5}$ and TSP samples were collected with a miniVol sampler (Airmetrics, Springfield, OR, USA) on 47 mm Whatman quartz-fiber filters (QM-A, Whatman, Clifton, NJ, USA) from August 11–17, 2004, and operated at a flow rate of $5 \text{ L}\cdot\text{min}^{-1}$ (Cao et al., 2003; 2005). TSP samples were also collected concurrently inside and outside of the museum. In addition to $\text{PM}_{2.5}$, size-segregated samples were collected on Whatman QM-A filters using an eight-stage Andersen cascade impactor (Thermo Electron Corporation, Burlington, Ontario, Canada) for particle diameters of 0.43, 1.1, 2.1, 3.3, 4.7, 5.8, 9, and $10 \mu\text{m}$ operated at flow rates of $28.3 \text{ L}\cdot\text{min}^{-1}$ at Pit 1. A portable Q-Trak monitor (Model 8551, TSI Inc., Shoreview, MN, USA) measured the average temperature, relative humidity (RH), and carbon dioxide (CO_2) concentrations on August 11, 15 and 16 at 5-minute intervals.

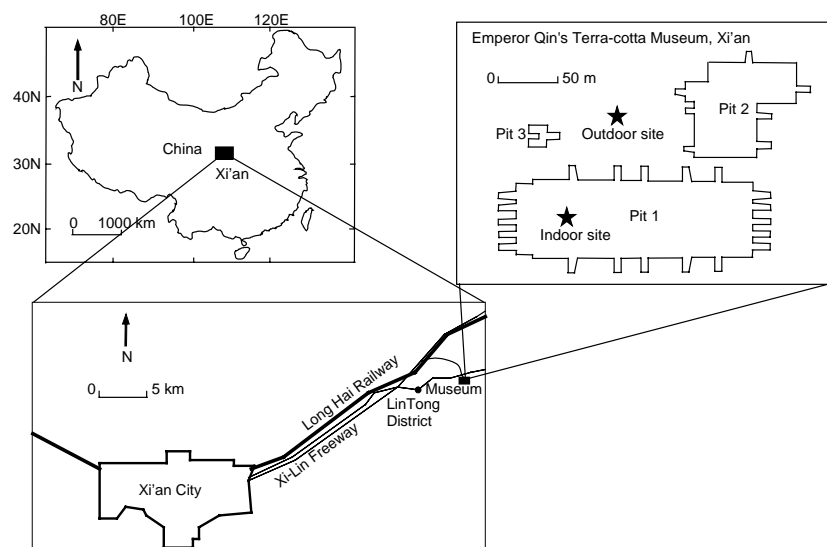


Fig. 1 Locations of the sampling sites inside and outside of the Museum of Qin Terra-Cotta Warriors and Horses in Xi'an, China.

Quartz-fiber filters were pre-heated at 900°C for 3 hours to remove the residual carbon content. Twenty-four-hour sampling was conducted each day with miniVol samplers, while on August 11, 13 and 15 with the Andersen cascade impactors.

2.2 Mass analyses

Quartz-fiber filters were analyzed gravimetrically for mass concentrations by means of a Sartorius MC5 electronic microbalance with a $\pm 1 \mu\text{g}$ sensitivity (Sartorius, Göttingen, Germany). These filters were weighed after 24-hour equilibration at temperature between 20°C, and 23°C and RH between 35% and 45%. Each filter was weighed at least three times before and after sampling, and the net mass was obtained by subtracting the difference between the averaged pre- and post-sampling weights. Precisions of the weighings were $<10 \mu\text{g}$ for blank filters and $<20 \mu\text{g}$ for filter samples.

2.3 Elemental analyses

The samples were analyzed for 17 elements (S, Cl, K, Ti, V, Cr, Mn, Fe, Ni, Cu, Zn, As, Se, Br, Sr, Zr, and Pb) by PIXE (Proton-induced X-ray emission spectroscopy) using 2.5 MeV protons with a 10 nA beam current through a 1.7 MV \times 2 MV accelerator at Beijing Normal University. The PIXE system was calibrated using the standards produced by MicroMatter Co. (Cao et al., 2005). Blank filter background spectra were subtracted prior to peak integration. Analysis of eight samples of standard reference materials in the National Bureau of Chemical Exploration Analysis, China (GSS, 1984), showed that reasonable precision ($<10\%$) and accuracy ($<15\%$) were achieved.

2.4 Organic carbon and elemental carbon analyses

Portions of the samples were analyzed for organic car-

bon (OC) and elemental carbon (EC) using a Desert Research Institute (DRI, Reno, NV, USA) Model 2001 thermal/optical carbon analyzer (Atmoslytic Inc., Calabasas, CA, USA). Quality assurance/quality control (QA/QC) procedures are described in Cao et al. (2003).

2.5 Ionic analyses

One quarter of a sample filter was extracted in 10 mL of high-purity water. Twelve major ionic species (Na^+ , NH_4^+ , K^+ , Mg^{2+} , Ca^{2+} , Sr^{2+} , F^- , Cl^- , NO_2^- , NO_3^- , Br^- and SO_4^{2-}) were measured by DX600 ion chromatography (Dionex Inc., Sunnyvale, CA, USA) (Chow & Watson, 1999). A CS12 column (150 mm \times 4 mm) and an AS14 column (150 mm \times 4 mm) were used for cation and anion analysis, respectively. The concentrations of ionic species were corrected by field blanks. The minimum detection limits (MDLs) were $15 \mu\text{g}\cdot\text{L}^{-1}$ for Na^+ , NH_4^+ , K^+ , Mg^{2+} , Ca^{2+} , and NO_3^- ; $0.5 \mu\text{g}\cdot\text{L}^{-1}$ for Sr^{2+} , F^- , Cl^- , NO_2^- , and Br^- ; and $20 \mu\text{g}\cdot\text{L}^{-1}$ for SO_4^{2-} and Cl^- . Six ions (NH_4^+ , K^+ , Mg^{2+} , Ca^{2+} , NO_3^- , and SO_4^{2-}) were detected in over 100% of the samples, with the other ions being 65% below MDLs. Ten percent of the samples were submitted for replicate analyses. Relative standard deviations of replicate analyses were 0.6%–2.5% for NO_3^- , 0.04%–2.3% for SO_4^{2-} , 1.4%–1.8% for NH_4^+ , and 2.3%–3.6% for K^+ , 0.7%–3.2% for Mg^{2+} , and 0.5%–2.1% for Ca^{2+} .

3. Results and Discussion

3.1 Microclimate

During the study, the indoor temperature fluctuation ranged from 3.2°C on August 15, to 5.1°C on August 11, and to 8.0°C on August 16. The daily average indoor temperature was 26.2°C, ranging from 21.9°C to 32.4°C. The maximum temperature of 32°C was recorded from

13:40 to 15:40 on August 11 as a result of solar radiation penetrating through the glass ceiling of the museum. The indoor RH oscillated daily between 56% and 80%, with an average of 70.8%, consistent with those reported by Zhang (1997). Even though the museum is located in a semi-arid region of China, with an annual precipitation of 550 mm, the indoor RH still reaches 70% during summer. These levels are 15%–20% higher than those measured at the Sainsbury Centre for Visual Arts, UK (Brimblecombe et al., 1999), and Correr museum, Italy (Camuffo et al., 1999). Higher temperatures and RH, along with solar radiation, tend to accelerate aerosol chemical reactions.

3.2 Aerosol chemical composition

PM_{2.5} concentrations are summarized in Table 1. The in-

door PM_{2.5} ranged from 53.2 $\mu\text{g}\cdot\text{m}^{-3}$ to 147.7 $\mu\text{g}\cdot\text{m}^{-3}$ with an average of 108.4 $\mu\text{g}\cdot\text{m}^{-3}$. The indoor TSP ranged from 92.7 $\mu\text{g}\cdot\text{m}^{-3}$ to 232.6 $\mu\text{g}\cdot\text{m}^{-3}$ with an average of 172.4 $\mu\text{g}\cdot\text{m}^{-3}$. The percentage of PM_{2.5} in TSP varied from 57.4% to 66.2%, with an average of 62.9%. This indicates that more than half of the TSP mass was associated with the fine particle (PM_{2.5}) mode. Most of the daily PM_{2.5} concentrations exceeded the 65 $\mu\text{g}\cdot\text{m}^{-3}$ of U.S. National Ambient Air Quality Standards (NAAQS), implying occurrence of high PM pollution in the museum even during summer, typically during the low outdoor PM pollution period. Larger variations of TSP were found outdoors than indoors, ranging from 68.5 $\mu\text{g}\cdot\text{m}^{-3}$ to 414.1 $\mu\text{g}\cdot\text{m}^{-3}$.

Table 1 Statistical summary of 24-hour PM_{2.5} and TSP chemical composition for samples acquired over eight days from August 11 through 17, 2004, indoors and outdoors at the Museum of Qin Terra-Cotta Warriors and Horses in Xi'an, China

	Indoor PM _{2.5}			Indoor TSP			Outdoor TSP		
	Mean	Max	Min	Mean	Max	Min	Mean	Max	Min
Mass	108.4	147.7	53.2	172.4	232.6	92.7	226.0	414.1	68.5
OC	17.6	21.3	15.1	23.9	29.7	18.7	26.8	33.4	25.2
EC	3.9	4.9	3.1	5.4	6.9	3.8	6.6	8.4	6.1
NH ₄ ⁺	10.3	16.1	1.5	10.9	18.0	1.7	6.6	11.5	0.3
NO ₃ ⁻	8.0	14.7	1.6	11.8	20.5	2.4	13.5	25.8	1.3
SO ₄ ²⁻	36.6	57.2	10.4	43.1	72.7	12.1	36.4	62.0	6.3
K ⁺	1.1	1.6	0.6	1.5	2.3	0.7	1.6	3.0	0.1
Mg ²⁺	0.1	0.2	0.0	0.4	0.7	0.2	0.9	2.0	0.1
Ca ²⁺	1.5	2.4	0.9	4.7	6.0	2.7	9.5	23.1	2.9
S	10.4	15.3	2.8	12.9	20.6	4.0	11.6	19.3	1.6
Cl	0.3	0.5	0.1	0.5	0.8	0.3	1.2	2.4	0.1
K	0.9	1.7	0.5	1.4	1.7	0.9	1.6	2.8	0.2
Tl	65.2	101.0	35.3	234.5	434.6	137.0	305.3	511.9	51.3
V	4.4	8.5	0.5	7.8	15.0	0.6	10.9	18.1	0.6
Cr	7.1	28.5	— ^b	6.7	9.3	1.9	5.5	13.9	— ^b
Mn	35.5	63.3	21.6	55.4	67.0	36.8	96.3	150.8	8.6
Fe	459.3	674.3	239.8	1707.6	2215.9	1180.3	2842.6	5510.7	316.7
Ni	6.4	16.0	— ^b	21.7	36.5	13.3	31.8	63.0	3.6
Cu	7.3	8.9	2.8	12.1	13.8	10.8	16.3	24.1	8.6
Zn	305.0	564.1	101.8	378.3	672.5	159.2	728.8	1809.0	41.3
As	19.8	32.2	13.6	18.3	45.0	— ^b	24.7	46.4	5.4
Se	11.6	19.8	0.6	14.5	28.1	— ^b	24.9	53.0	1.5
Br	14.1	39.1	— ^b	14.3	31.2	— ^b	23.7	72.7	4.4
Sr	10.3	25.2	— ^b	43.3	58.3	20.1	44.9	83.8	9.0
Zr	127.9	187.3	75.6	126.7	183.3	56.7	111.5	166.0	37.7
Pb	154.0	286.1	69.3	204.3	318.1	79.2	287.0	626.2	35.8

^aUnit: from mass to K, $\mu\text{g}\cdot\text{m}^{-3}$; from Ti to Pb, $\text{ng}\cdot\text{m}^{-3}$. ^b—: the value was under the detection limit.

3.2.1 Organic and elemental carbon

Average OC concentrations for indoor PM_{2.5} and TSP were 17.6 $\mu\text{g}\cdot\text{m}^{-3}$ and 23.9 $\mu\text{g}\cdot\text{m}^{-3}$, and the corresponding average EC concentrations were 3.9 $\mu\text{g}\cdot\text{m}^{-3}$ and 5.4 $\mu\text{g}\cdot\text{m}^{-3}$ (Table 1). The indoor PM_{2.5} OC and EC concentrations varied by 1.5-fold, ranging from 15.1 $\mu\text{g}\cdot\text{m}^{-3}$ to 21.3 $\mu\text{g}\cdot\text{m}^{-3}$ and 3.1 $\mu\text{g}\cdot\text{m}^{-3}$ to 4.9 $\mu\text{g}\cdot\text{m}^{-3}$, respectively. Similar differences were found for indoor TSP carbon. The average OC and EC concentrations for outdoor TSP were 26.7 $\mu\text{g}\cdot\text{m}^{-3}$ and 6.6 $\mu\text{g}\cdot\text{m}^{-3}$, respectively. Indoor TSP EC concentrations are comparable to those at Sepulveda House (5.6 $\mu\text{g}\cdot\text{m}^{-3}$), but are higher than those at the Norton Simon

Museum (0.67 $\mu\text{g}\cdot\text{m}^{-3}$) and Scott Gallery (0.16 $\mu\text{g}\cdot\text{m}^{-3}$) in Southern California (Nazaroff et al., 1990).

The OC/EC ratios for indoor PM_{2.5} varied between 4.0 and 4.8 with an overall average of 4.5, which is similar to the indoor (3.9 to 5.3) and outdoor (4.0 to 4.1) TSP ratios. Since 89% of the OC and 82% of the EC outdoors were found indoors, elevated concentrations in the museum are affected mainly by outdoor sources. The museum is located in a rural village of Xi'an where there are few carbon emission sources except for biomass burning during harvest periods. The observed OC/EC ratios are typical of urban ratios (Gray et al., 1986) and are probably due to transport from nearby Xi'an.

3.2.2 Water-soluble ions

SO_4^{2-} contributions were the highest of the ionic species with an average of $36.6/43.1 \mu\text{g}\cdot\text{m}^{-3}$ for indoor $\text{PM}_{2.5}/\text{TSP}$. Compared with the observations of Santis et al. (1992), SO_4^{2-} , NO_3^- , and NH_4^+ inside Xi'an museum were approximately 4 fold, 7 fold, and 8 fold, respectively, higher than those at Galleria degli Uffizi in Florence, Italy.

Equations (1) and (2) are used to calculate the charge balance between cations and anions. The correlations between cations and anions are shown in Fig. 2.

$$\text{Cation equivalence} = \frac{\text{Ca}^{2+}}{20} + \frac{\text{K}^+}{39} + \frac{\text{Mg}^{2+}}{12} + \frac{\text{NH}_4^+}{18}, \quad (1)$$

$$\text{Anion equivalence} = \frac{\text{NO}_3^-}{62} + \frac{\text{SO}_4^{2-}}{48}. \quad (2)$$

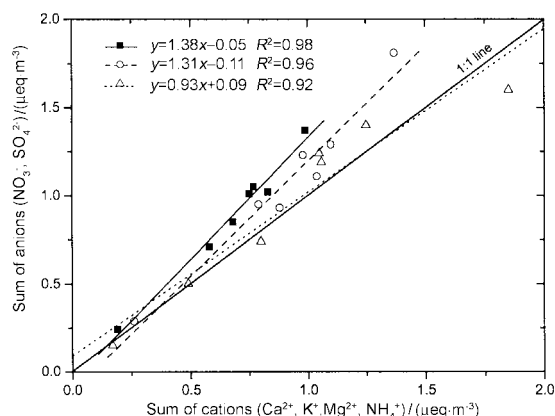


Fig. 2 Cation and anion balance in indoor $\text{PM}_{2.5}$ and indoor/outdoor TSP.

The cation and anion concentrations measured for indoor $\text{PM}_{2.5}/\text{TSP}$ and outdoor TSP have correlation coefficients greater than 0.95, suggesting a common origin. The slopes of indoor $\text{PM}_{2.5}$ and TSP (Fig. 2) are close to 1.3. Since most inorganic species have been measured, the deficits of cation species indoors is consistent with the presence of hydrogen ions (H^+), implying that the particles are acidic (Kerminen et al., 2001). Acidic aerosol in the museum can greatly damage antiques. The slope 0.93 of outdoor TSP is close to 1.0, consistent with cation species being neutralized in the outdoor atmosphere. High concentrations of Ca^{2+} in coarse mode contribute to the neutralization of excess sulfuric and nitric acidic particles (Table 1).

3.2.3 Elemental composition

The highest concentration of the 17 elements was sulfur, in cases of both indoors and outdoors, pointing to the heavy influence of anthropogenic sources. The average S concentration in TSP reached $12.9 \mu\text{g}\cdot\text{m}^{-3}$, which is 6 to 60 times higher than the S concentrations in four European museums (Camuffo et al., 2001). Enrichment factors of each element are shown in Fig. 3 relative to crustal rock using Fe (Taylor & McLennan, 1985) as a reference element.

$$\text{EF} = (\text{X}/\text{Fe})_{\text{air}} / (\text{X}/\text{Fe})_{\text{crust}}, \quad (3)$$

where EF is the enrichment factor of element X, $(\text{X}/\text{Fe})_{\text{air}}$ is

the concentration ratio of X to Fe in the aerosol samples, and $(\text{X}/\text{Fe})_{\text{crust}}$ is the average concentration ratio of X to Fe in crustal rock. Fe is used because it is a good indicator of the presence of crustal material and is less affected by contamination than other elements.

If EF-value approaches unity, suspended dust is probably the predominant source for element X. Figure 3 shows that EF_{crust} values for Mn, Sr, K, Ti, and Cr are all close to unity with maximum values less than 5, indicating that these elements were dominated by mineral dust. Compared to the dust-derived elements, the EF values for Se, S, As, Pb, Zn, Zr, Cu, Ni, and V are much larger than 5, illustrating the influence of anthropogenic sources such as industrial activities (Zn, Cu, S), coal-combustion (Se, As, S), oil combustion (Ni, V, S) and motor vehicle exhaust (Pb, Zn). Se, S and As are the highest enriched elements. These high EF-values, ranging from 10^3 to 10^5 , were found for Se, S, and As, consistent with coal-burning emissions (Zhang et al., 2002). A major coal-fired power plant (i.e., Baqiao Redian Factory) is located ~15 km east of the museum and emitted 1.6 tons of soot per day. Average EFs for Pb and Zn in the range of 10 to 10^3 are related to motor vehicle exhausts. All the EF-values of anthropogenic elements associated with the indoor $\text{PM}_{2.5}$ are large than those with the indoor TSP (Fig. 3), implying presence of these elements in fine particles.

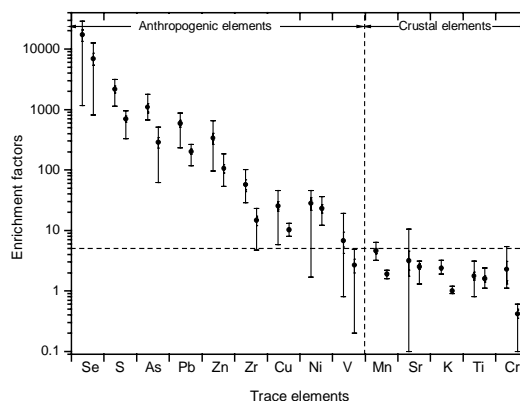


Fig. 3 Enrichment factor (EF) of 14 abundant trace elements in indoor aerosol samples. (The left boxplot of each pair EFs for an element refers to the EFs in $\text{PM}_{2.5}$ and the right boxplot refers to the EFs in TSP.)

3.3 Material balances of $\text{PM}_{2.5}$ and TSP

The material balance approach (Solomon et al., 1989) is used to estimate mass closure, since PIXE data does not analyze Al and Si. Fe is used to estimate the upper limit of geological material (Taylor & McLennan, 1985). The amount of geological material was calculated by

$$\text{Geological material} = (1/0.035) \times \text{Fe}. \quad (4)$$

The amount of organic material was determined by multiplying the amount of OC by 1.6 according to Turpin and Lim (2001):

$$\text{Organic material} = 1.6 \times \text{OC}. \quad (5)$$

The material balances for geological material (crustal material), organics, EC, ammonium (NH_4^+), sulfate (SO_4^{2-}),

nitrate (NO_3^-) and others (as the difference between the measured mass and the sum of the major components) for indoor $\text{PM}_{2.5}$ /TSP and outdoor TSP, are shown in Fig. 4. SO_4^{2-} was the largest component of indoor $\text{PM}_{2.5}$, accounting for $(32.4 \pm 6.2)\%$ of the mass. However, geological material was most abundant in TSP, accounting for $(29.0 \pm 3.7)\%$ indoors and $(33.5 \pm 9.1)\%$ outdoors. Organic material was the second important component for indoor and outdoor samples, with an average of 27.7% for the indoor $\text{PM}_{2.5}$, 23.0% for the indoor TSP, and 24.3% for the outdoor TSP. EC constituted 3%–4% of indoor $\text{PM}_{2.5}$ /TSP and outdoor TSP. Total carbonaceous aerosol (TCA, the sum of organic material and EC) accounted for approximately one-third of indoor $\text{PM}_{2.5}$, and more than one fourth of indoor/outdoor TSP. A major freeway from Xi'an to other eastern cities of Shaanxi province is 10 km away from the museum (Fig. 1). The fraction of NH_4^+ decreased from $(8.9 \pm 2.8)\%$ for the indoor $\text{PM}_{2.5}$ to $(6.0 \pm 1.9)\%$ for the indoor TSP, to $(2.7 \pm 1.8)\%$ outdoor TSP. A high portion of NH_4^+ in $\text{PM}_{2.5}$ is largely due to the neutralization of gaseous ammonia (NH_3) by sulfuric and nitric acids. Elevated NH_3 may be associated with use of fertilizers in the farmland around the museum as well as contributions from local sanitation waste. Additional ammonia indoors can be attributed to NH_3 from 5000 tourists per day and from un-vented indoor restrooms. NO_3^- accounted for around 5%–7% of indoor $\text{PM}_{2.5}$ and indoor/outdoor TSP, that can be attributed to the influence of motor vehicles.

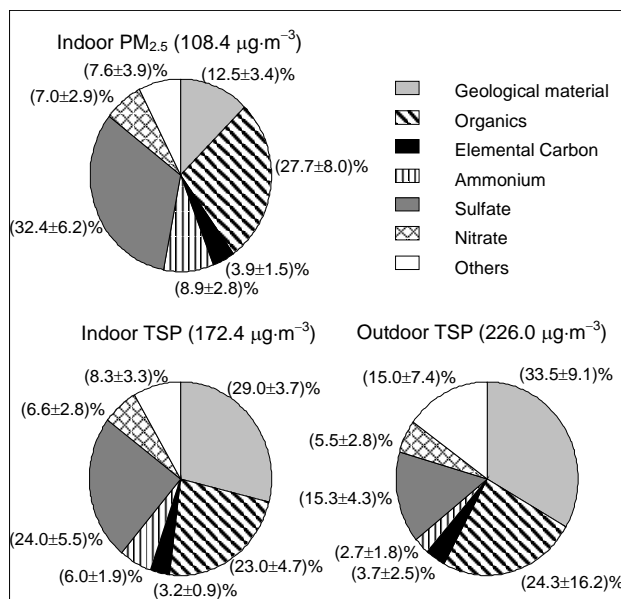


Fig. 4 Material balance charts for indoor $\text{PM}_{2.5}$ and indoor/outdoor TSP.

During the pilot study, $\text{PM}_{2.5}$ and TSP mass concentrations varied 2–3 fold, as shown in Fig. 5. The increased $\text{PM}_{2.5}$ mass indoors was mostly due to increases in secondary inorganic aerosol (e.g., SO_4^{2-} , NH_4^+ , and NO_3^-). Sharp decreases of $\text{PM}_{2.5}$ mass of $94.5 \mu\text{g}\cdot\text{m}^{-3}$ from Au-

gust 11 to 12 can be attributed to SO_4^{2-} ($46.8 \mu\text{g}\cdot\text{m}^{-3}$), NH_4^+ ($14.6 \mu\text{g}\cdot\text{m}^{-3}$), and NO_3^- ($9.4 \mu\text{g}\cdot\text{m}^{-3}$), which accounted for 75.0% of the decreased mass. In contrast, the geological material and SO_4^{2-} were the dominant components contributed to the increased mass in TSP.

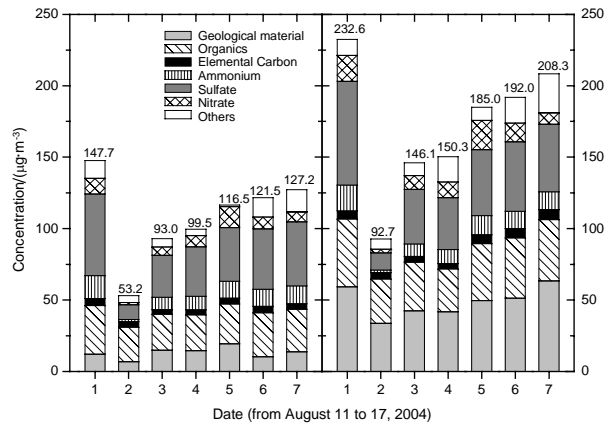


Fig. 5 Weekly variations of each chemical component from August 11 to 17.

3.4 Size-differentiated characterization of indoor aerosol

Size-differentiated concentrations of mass, OC, EC, NH_4^+ , SO_4^{2-} , and NO_3^- indoors are shown in Fig. 6. The smooth curves of mass shown in the figure represent the midpoints of each bar. A bimodal mass size distribution is shown with one peak in the fine mode ($2.5 \mu\text{m}$) and another in the coarse mode ($10 \mu\text{m}$). The fine mode is the dominant fraction, contributing 58.9%, 54.3%, and 62.3% to the total mass of aerosols on August 11, 13, and 15, respectively. This is comparable to the ratio of $\text{PM}_{2.5}$ in TSP, 63.5%, 59.5%, and 63.0%, respectively, on these days.

It is evident from Fig. 6 that the fine mode (stage 1–4) is composed primarily of OC, EC, NH_4^+ , SO_4^{2-} , and NO_3^- . On average, the sum of these species comprised per stage 92.9% (1), 71.9% (2), 86.6% (3), 72.5% (4), 49.7% (5), 53.3% (6), 54.9% (7), 29.8% (8), and 19.2% (9) of the mass. The coarse fraction (stage 5 to 9) is mainly associated with geological materials.

Except for organic compounds, the EC, NH_4^+ , SO_4^{2-} , and NO_3^- were found to have a unimodal distribution. A large fraction of SO_4^{2-} , NO_3^- , and NH_4^+ is found in the fine mode, showing a peak in the range of 1.1–3.3 μm . A high SO_4^{2-} fraction in fine mode is consistent with the observation of Gysels et al. (2002) in the Royal Museum of Fine Arts, Belgium. It is generally assumed that the NH_4^+ ion is predominantly associated with SO_4^{2-} and NO_3^- in the atmosphere. If all particulate NH_4^+ , NO_3^- , and SO_4^{2-} were presented as ammonium nitrate (NH_4NO_3) and ammonium sulfate [$(\text{NH}_4)_2\text{SO}_4$], then the ratio, $\text{neq}[\text{NH}_4^+] = (\text{neq}[\text{SO}_4^{2-}] + \text{neq}[\text{NO}_3^-])$ would be equal to unity. This ratio was calculated for each sample. Their average ratios ranged between 0.4 and 0.7 by the fine mode and between 0.4 and

0.6 by the coarse mode. This indicated that NH_4^+ ions insufficient to neutralize the nitric and sulphuric acids, resulting in the acidic nature of indoor aerosols. Gysels et al. (2002) showed that organic compounds, S-rich and Fe-rich particles with a diameter around $0.5 \mu\text{m}$, are considered as the most harmful factor to the works of art in a museum.

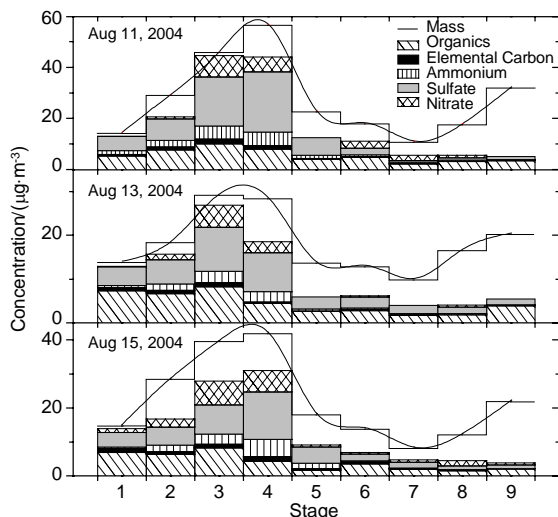


Fig. 6 Size distribution of the differential aerosol mass and concentrations of chemical components in the samples on August 11, 13, 15, 2004. [(Stage 1: $<0.43 \mu\text{m}$, stage 2: $0.43\text{--}1.1 \mu\text{m}$, stage 3: $1.1\text{--}2.1 \mu\text{m}$, stage 4: $2.1\text{--}3.3 \mu\text{m}$, stage 5: $3.3\text{--}4.7 \mu\text{m}$, stage 6: $4.7\text{--}5.8 \mu\text{m}$, stage 7: $5.8\text{--}9.0 \mu\text{m}$, stage 8: $9.0\text{--}10.0 \mu\text{m}$, stage 9: $>10 \mu\text{m}$).

4. Conclusions

The chemical compositions of aerosol in the Emperor Qin's Terra-cotta Museum, Xi'an, China were investigated through a short-term campaign during the summer, 2004. High concentrations of PM and its associated chemicals were measured inside and outside of the museum. High concentrations of acidic aerosols will erode the surface of Terra-cotta warriors and horses especially under high temperature (30°C) and relative humidity (70%) with solar radiation increasing. While the characterization of indoor aerosols has begun, further work is needed to address issues such as long-term variations of indoor/outdoor aerosols and gaseous oxidants, as well as their potential impact on terra-cotta antiquities to gain insight into the damage mechanisms of air pollutants on the cultural relics.

Acknowledgement

This project is supported by the National Natural Science Foundation of China (NSFC 40205018, 40121303), and also supported by Ministry of Science and Technology (2004CB720203).

References

Baer, N. S. & Banks, P. N. (1985). Indoor air pollution: effects on cultural and historical materials. *Int. J. Museum Manage. Curatorship*, 4, 9–20.
 Brimblecombe, P. (1990). Review article: the composition of museum atmospheres. *Atmos. Environ.*, 24, 1–8.
 Brimblecombe, P., Blades, N., Camuffo, D., Sturaro, G., Valentino, A., Gysels, K., van Grieken, R., Busse, H. J., Kim, O., Ulrych, U.

& Wieser, M. (1999). The indoor environment of a modern museum building; The Sainsbury Centre for Visual Arts Norwich UK. *Indoor Air*, 9, 146–164.
 Camuffo, D., Brimblecombe, P., van Grieken, R., Busse, H. J., Sturaro, G., Valentino, A., Bernardi, A., Blades, N., Shooter, D., De Bock, L., Gysels, K., Wieser, M. & Kim, O. (1999). Indoor air quality at the Correr Museum, Venice, Italy. *Sci. Total Environ.*, 236, 135–152.
 Camuffo, D., Grieken, R. V., Busse, H. J., Sturaro, G., Valentino, A., Bernardi, A., Blades, N., Shooter, D., Gysels, K. & Deutsch, F. (2001). Environmental monitoring in four European museums. *Atmos. Environ.*, 35, S127–S140.
 Cao, J. J., Lee, S. C., Ho, K. F., Zou, S. C., Zhang, X. Y. & Pan, J. G. (2003). Spatial and seasonal distributions of atmospheric carbonaceous aerosols in Pearl River Delta Region, China. *China Particology*, 1(1), 33–37.
 Cao, J. J., Lee, S. C., Zhang, X. Y., Chow, J. C., An, Z. S., Ho, K. F., Watson, J. G., Fung, K., Wang, Y. Q. & Shen, Z. X. (2005). Characterization of airborne carbonate over a site on Asian dust source regions during 2002 spring and its climatic and environmental significance. *J. Geophys. Res.*, 110, D03203, doi:10.1029/2004JD005244.
 Chow, J. C. & Watson, J. G. (1999). Ion chromatography in elemental analysis of airborne particles. In Landsberger, S. & Creatchman, M. (Eds.), *Elemental Analysis of Airborne Particles*, Vol.1 (pp.97–137). Amsterdam: Gordon and Breach Science.
 De Bock, L., van Grieken, R., Camuffo, D. & Grime, G. W. (1996). Microanalysis of museum aerosols to elucidate the soiling of paintings: case of the Correr Museum, Venice, Italy. *Environ. Sci. Technol.*, 30, 3341–3350.
 Gray, H. A., Cass, G. R., Huntzicker, J. J., Heyerdahl, E. K. & Rau, J. A. (1986). Characteristics of atmospheric organic and elemental carbon particle concentrations in Los Angeles. *Environ. Sci. Technol.*, 20(6), 580–589.
 GSS (1984). *Preparation of Geochemical Standard References Samples* (GSR1-6, GSS1-8, GSD9-12). Beijing: National Bureau of Chemical Exploration Analysis.
 Gysels, K., Deutsch, F. & Grieken, R. V. (2002). Characterization of particulate matter in the Royal Museum of Fine Arts, Antwerp, Belgium. *Atmos. Environ.*, 36, 4103–4113.
 Kerminen, V. M., Hillamo, R., Teinila, K., Pakkanen, T., Allegrini, I. & Sparapani R. (2001). Ion balances of size-resolved tropospheric aerosol samples: implications for the acidity and atmospheric processing of aerosols. *Atmos. Environ.*, 35, 5255–5265.
 Nazaroff, W. M., Salmon, L. G. & Cass, G. R. (1990). Concentration and fate of airborne particles in museums. *Environ. Sci. Technol.*, 24, 66–77.
 Oddy, W. A. (1994). Chemistry in the conservation of archaeological materials. *Sci. Total Environ.*, 143, 121–126.
 Santis, F. D., Palo, V. D. & Allegrini, I. (1992). Determination of some atmospheric pollutants inside a museum: relationship with the concentration outside. *Sci. Total Environ.*, 127, 211–223.
 Solomon, P. A., Fall, T., Salmon, L., Cass, G. R., Gray, H. A. & Davidson, A. (1989). Chemical characteristics of PM_{10} aerosols collected in the Los Angeles Area. *J. Air Pollut. Control Assoc.*, 39, 154–163.
 Taylor, S. R. & McLennan, S. M. (1985). *The Continental Crust: its Composition and Evolution* (p.315). Oxford: Blackwell.
 Turpin, B. J. & Lim, H. J. (2001). Species contributions to $\text{PM}_{2.5}$ mass concentrations: revisiting common assumptions for estimating organic mass. *Aerosol Sci. Technol.*, 35, 602–610.
 Zhang, X. Y., Cao, J. J., Li, L. M., Arimoto, R., Cheng, Y., Huebert, B. & Wang, D. (2002). Characterization of atmospheric aerosol over Xi'an in the south margin of the Loess Plateau, China. *Atmos. Environ.*, 36, 4189–4199.
 Zhang, Z. J. (1997). Study on environmental quality of Emperor Qin's Terra-cotta Museum, Xi'an. In Zhang, Z. J. (Ed.), *Conservation of Terra-cotta Warriors and Horses* (pp.1–49). (in Chinese)

Manuscript received January 26, 2005 and accepted March 2, 2005.